Predicting pressure gradient using artificial intelligence for transcatheter aortic valve replacement

Anoushka Dasi, BS,[a] Beom Lee, MS,[b] Venkateshwar Polsani, MD, FACC, FASE,[c] Pradeep Yadav, MD, FACC,[c] Lakshmi Prasad Dasi, PhD, FACC, FAIMBE,[b] and Vinod H. Thourani, MD, FACS, FACC[c]

ABSTRACT

Objective: After transcatheter aortic valve replacement, the mean transvalvular pressure gradient indicates the effectiveness of the therapy. The objective is to develop artificial intelligence to predict the post–transcatheter aortic valve replacement aortic valve pressure gradient and aortic valve area from preprocedural echocardiography and computed tomography data.

Methods: A retrospective study was conducted on patients who underwent transcatheter aortic valve replacement due to aortic valve stenosis. A total of 1091 patients were analyzed for pressure gradient predictions (mean age 76.8 ± 9.2 years, 57.8% male), and 1063 patients were analyzed for aortic valve area predictions (mean age 76.7 ± 9.3 years, 57.2% male). An artificial intelligence learning model was trained (training: n = 663 patients, validation: n = 206 patients) and tested (testing: n = 222 patients) to predict pressure gradient, and a separate artificial intelligence learning model was trained (training: n = 640 patients, validation: n = 218 patients) and tested (testing: n = 205 patients) for predicting aortic valve area.

Results: The mean absolute error for pressure gradient and aortic valve area predictions was 3.0 mm Hg and 0.45 cm^2, respectively. Valve sheath size, body surface area, and age were determined to be the top 3 predictors for pressure gradient, and valve sheath size, left ventricular ejection fraction, and aortic annulus mean diameter were identified to be the top 3 predictors of post–transcatheter aortic valve replacement aortic valve area. A training dataset size of more than 500 patients demonstrated good robustness of the artificial intelligence models for pressure gradient and aortic valve area.

Conclusions: The artificial intelligence–based algorithm has demonstrated potential in predicting post–transcatheter aortic valve replacement transvalvular pressure gradient predictions for patients with aortic valve stenosis. Further studies are necessary to differentiate pressure gradient between valve types. (JTCVS Techniques 2024;23:5-17)

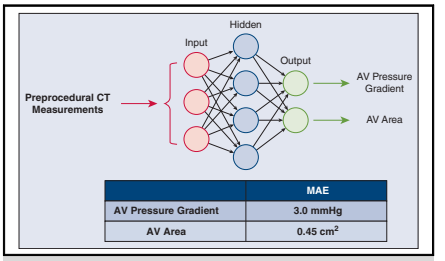

Implementing AI to predict AV pressure gradient and AVA.

CENTRAL MESSAGE

AI demonstrates potential in predicting postoperative transvalvular pressure gradient and AVA for patients undergoing TAVR.

PERSPECTIVE

AI can be used to predict the transvalvular pressure gradient and AVA after TAVR given preprocedural CT and echocardiography data. Including intraprocedural variables as input features can be investigated as a potential source of improvement for the learning algorithms. Prospective studies could be conducted to confirm the durability of these models.

Transcatheter aortic valve replacement (TAVR) is currently the most prevalent form of valve therapy for patients diagnosed with aortic stenosis (AS) in the United States and is used as an alternative approach to surgical aortic valve replacement (SAVR).[1-3] Computed tomography (CT) is the primary means for evaluating the aortic valve (AV) and peripheral arterial vasculature. These preprocedural measurements are evaluated to aid the selection of the transcatheter heart valve prosthesis and femoral or alternative access sheath access.[4-6] Additional tools used to assess patients include surgical risk assessment models, such as the European System for Cardiac Operative Risk Evaluation I and II, and the Society of Thoracic Surgeons score, which apply statistical methods to predict postprocedural outcomes.[7]

A complication of TAVR includes patient-prosthesis mismatch (PPM), which is defined by an effective orifice area (EOA) of the prosthetic valve that is too small in

From the [a]Department of Biomedical Engineering, Ohio State University, Columbus, Ohio; [b]Department of Biomedical Engineering, Georgia Institute of Technology, Atlanta, Ga; and [c]Department of Cardiac Surgery, Piedmont Heart Institute, Atlanta, Ga.

Received for publication July 30, 2023; revisions received Oct 29, 2023; accepted for publication Nov 9, 2023; available ahead of print Nov 30, 2023.

Address for reprints: Vinod H. Thourani, MD, FACS, FACC, Department of Cardiovascular Surgery, Piedmont Heart Institute, 95 Collier Rd Suite 5015, Atlanta, GA 30309 (E-mail: vinod.thourani@piedmont.org).

2666-2507

https://doi.org/10.1016/j.xjtc.2023.11.011

Abbreviations and Acronyms

AI = artificial intelligence
ANN = artificial neural network
AS = aortic stenosis
AV = aortic valve
AVA = aortic valve area
BMI = body mass index
BSA = body surface area
CT = computed tomography
EOA = effective orifice area
EOAI = effective orifice area index
GBM = gradient boosting machine
IQR = interquartile range
LVEF = left ventricular ejection fraction
MAE = mean absolute error
ML = machine learning
PPM = patient-prosthesis mismatch
SAVR = surgical aortic valve replacement
STJ = sinotubular junction
SVR = support vector regression
TAVR = transcatheter aortic valve replacement

relation to the patient body surface area (BSA).[8] Specifically, moderate PPM is identified by an effective orifice area index (EOAI) threshold less than 0.85 cm^2/m^2, and severe PPM is defined by EOAI values less than 0.65 cm^2/m^2 for a body mass index (BMI) less than 30 kg/m^2. For BMI values greater than 30 kg/m^2, the moderate and severe PPM thresholds are set at less than 0.7 cm^2/m^2 and 0.55 cm^2/m^2, respectively.[8]

Based on echocardiographic measurements conducted on patients with nonmechanical prostheses, the EOAI threshold corresponds to a postoperative residual transvalvular pressure gradient greater than or equal to 10 mm Hg.[9] PPM risk factors include older age, female sex, higher BSA and BMI values, diabetes, hypertension, and receiving a bioprosthetic valve instead of a mechanical prosthesis.[10] Regarding the clinical impact of postoperative echocardiographic gradients and PPM, recent findings have demonstrated little to no association between post-TAVR echocardiographic pressure gradients and mortality according to a multicenter retrospective registry of patients undergoing TAVR.[11] Additionally, a study that conducted a PARTNER 3 trial to compare postprocedural echocardiographic measurements for patients with severe AS after SAVR versus TAVR reported no correlation between severe PPM and 1-year mortality.[12] Although these findings indicate an unclear relationship among the transvalvular pressure gradient, PPM, and patient outcomes, it remains preferable to prevent the occurrence of PPM and minimize the pressure gradient by calculating its incidence based on the preprocedural CT measurements and the anticipated transcatheter heart valve prosthesis.[13,14]

Current predictive tools used for cardiovascular procedures, in general, include the application of machine learning (ML) and artificial intelligence (AI)-based models to predict in-hospital mortality and occurrence of intraprocedural and postprocedural complications.[15-17] Specifically considering the development of predictive technology for TAVR, ML models, such as gradient boosting machine (GBM) algorithms, have been implemented to determine predictors of 1-year mortality and in-hospital mortality in patients with AS who underwent TAVR.[15,16] The main limitation of conventional predictive tools is the assumption that the data are normally distributed and that all variables considered are independent and hold a linear relationship with the predicted variable. In contrast, ML models function by analyzing the relationship between a given input dataset and its corresponding output variable by iteratively fitting an optimal linear or nonlinear function that allows the input to be mapped to its output.[18]

With ML and AI-based learning algorithms becoming more prevalent in predicting medical outcomes, we applied AI-based learning models to investigate the predictive ability of pre-TAVR CT and echocardiography measurements obtained from patients diagnosed with AS in estimating the postprocedural pressure gradient across the AV as well as the aortic valve area (AVA) measurements obtained using Doppler echocardiography. Obtaining accurate predictions of these values can provide insight into the impact of TAVR on the transvalvular pressure gradient and thus aid clinicians in adjusting the intraprocedural parameters to minimize the pressure gradient value.

MATERIAL AND METHODS

A retrospective study was conducted on patients with AS who have undergone TAVR from January 1, 2016, to December 27, 2021, at Piedmont Heart Institute, Atlanta, Georgia. Data analyzed for this study involve preprocedural CT measurements of the patients' vasculature and cardiac anatomy and Doppler-echocardiography measurements acquired pre- and post-TAVR. The features obtained from the CT data include diameter, perimeter, area, and height of the aortic annulus, sinotubular junction (STJ), sinus of Valsalva, coronary cusps, coronary ostia, peripheral arteries, and so forth, as well as calcium, stenosis, tortuosity, and dissection severity. Additional aspects of the data considered include patient history, initial AVA, age, BSA, and preprocedural echocardiography information, including pre-TAVR left ventricular ejection fraction (LVEF) and AV peak velocity. Additionally, procedural information, such as valve sheath size, access site, and access method, were set as variables. The echocardiography data include the post-TAVR mean transvalvular pressure gradient and AVA that we aim to predict given the preprocedural and intraprocedural data as the input. A complete list of all variables examined during this study is shown in Table E1.

Preprocessing

To ensure the optimal predictive performance of the resulting AI learning algorithm, the pre-TAVR dataset was first analyzed and preprocessed using python software (Google Colaboratory) by applying the following steps: removing specific features, determining numerical and

categorical features, performing the training-validation-test split, removing outlier values, imputing/feature scaling, and eliminating multicollinearity. A thorough description of these steps is provided in the Appendix E1 under the "Preprocessing Steps" section.

Learning Algorithm

A combination of regression and artificial neural network (ANN)-based AI learning models was trained and validated on 80% of the provided data and then applied to the remaining 20% testing data to obtain the final pressure gradient and AVA predictions (Figure 1). Specifically, the prediction methods implemented include elastic net regression, support vector regression (SVR), random forest regression, gradient boosting regressor, multilayer perceptron regressor or ANN, and voting regression.

For the elastic net, SVR, random forest, gradient boosting, and ANN algorithms, each model was iterated over an array of chosen sample values for variable hyperparameters, such as the regularization parameter and acceptable absolute error margin. These models were trained in this manner to identify the best combination of model hyperparameters that would yield the lowest error between the predicted and true pressure gradient or AVA. Definitions of the hyperparameters and detailed explanations about how the applied algorithms function are provided in the scikit-sklearn documentation as well as several additional resources provided in the Appendix E1 References. In addition, details surrounding the hyperparameters chosen and the range of values investigated for these variables can be found in the Appendix E1 under the "Hyperparameter Fine-tuning: Regression" section.

After the fine-tuning process, the voting regressor was trained to provide a final output by averaging the predictions outputted by the neural network and the best estimators determined for the SVR, elastic net, random forest, and gradient boosting models. This regression was performed to ensure the robustness of the final predictive model. The mean absolute error (MAE) between the predicted, and the true pressure gradient was calculated to assess the performance of each algorithm. By using the final voting regressor estimator, the top 10 variables with the strongest predictive ability were identified using a permutation-based feature importance function, which computes the increase in MAE following a permutation of an input variable.[19] This change in performance was measured relative to the MAE calculated before permuting the variables. A total of 10 different permutations were performed by the feature importance function to compute the mean increase in MAE for each input variable.

RESULTS

As shown in Table 1, a total of 1091 patients were analyzed for predicting pressure gradient (76.8 ± 9.2 years, 631 [57.8%] male). A total of 663 patients were used for training the learning models, and 206 and 222 patients were used for validation and testing, respectively. Implementing the learning algorithm yielded a final calculated MAE of 2.7 mm Hg and 3.0 mm Hg for the training and test set, respectively. The respective mean pressure gradients for the true and predicted output for the training set were computed to be 10.0 mm Hg and 9.7 mm Hg, and the calculated SDs for the true and predicted sets for the training data were 4.5 and 2.1, respectively. For the testing set, the mean values were 9.8 mm Hg and 9.7 mm Hg, and the SD values were 4.2 mm Hg and 1.9 mm Hg, respectively. The average 5th percentile and 95th percentile values from the prediction intervals output by the gradient boosting algorithm were

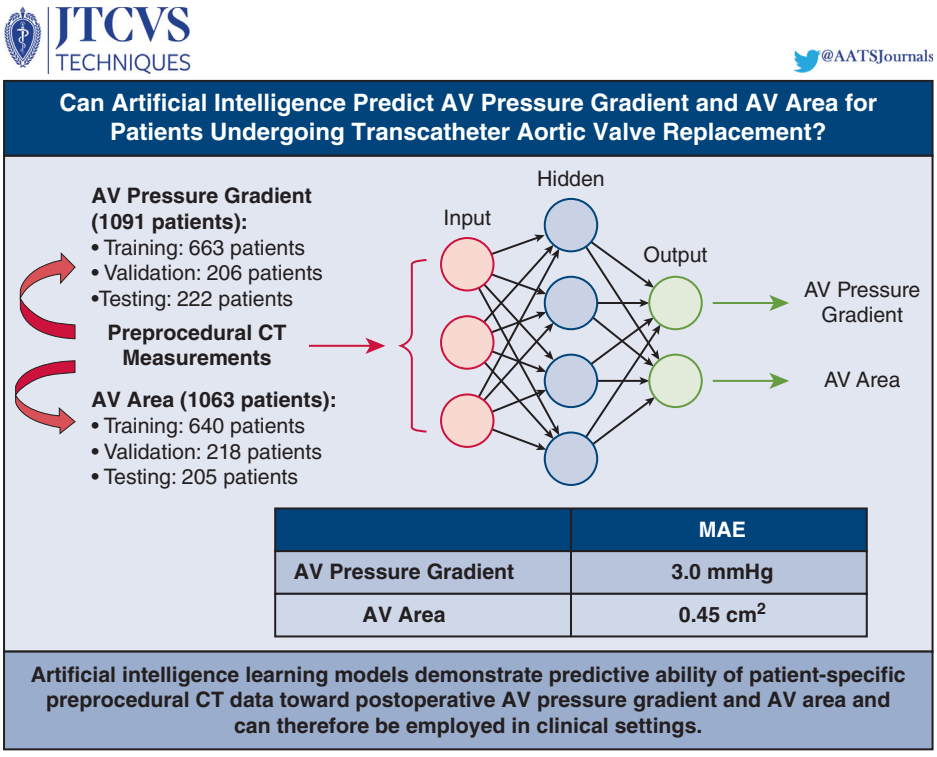

*AV = aortic valve, CT = computed tomography, MAE = mean absolute error

FIGURE 1. Implementing a combination of AI learning models to predict AV pressure gradient and AVA. *AV*, Aortic valve; *CT*, computed tomography; *MAE*, mean absolute error.

TABLE 1. Patients analyzed during study for pressure gradient and aortic valve area predictions

Variables	No. of patients	Age (y)	Gender	Train-validation-test split
Pressure gradient	1091	76.8 ± 9.2	631 M: 460 F	Train: 663 patients Validation: 206 patients Test: 222 patients
AV area	1063	76.7 ± 9.3	608 M: 455 F	Train: 640 patients Validation: 218 patients Test: 205 patients

AV, Aortic valve.

calculated to be 3.3 mm Hg and 18.5 mm Hg for both training and testing sets, respectively.

For AVA predictions, 1063 patients were analyzed (76.7 ± 9.3 years: 608 [57.2%] male). The training set consisted of 640 patients, and the validation and testing sets consisted of 218 and 205 patients, respectively. The final computed MAE values obtained from applying the learning algorithm were 0.40 cm^2 and 0.45 cm^2 for the training and test set, respectively. The mean values for the true and predicted output for the training set were calculated to be 1.94 cm^2 and 1.90 cm^2, and the SD values were 0.57 cm^2 and 0.15 cm^2, respectively. For the testing set, the mean values were 1.90 cm^2 for both the true and predicted sets, and the respective SD values were computed to be 0.59 cm^2 and 0.14 cm^2. The final prediction intervals obtained from the gradient boosting algorithm resulted in average 5th percentile and 95th percentile values computed to be 1.15 cm^2 and 2.96 cm^2 for both the training and testing sets, respectively.

Scatter plots of the predicted versus true pressure gradient were generated for both the training and test data as shown in Figure 2, *A* and *B*. The top 10 input variables with the highest calculated feature importance values for pressure gradient and AVA predictions were obtained using the voting regression algorithm. The results are displayed in Figure 3, *A* and *B*. The strongest predictors of AV pressure gradient were identified to be valve sheath size, BSA, and age with an average increase in MAE computed to be approximately 0.6, 0.2, and 0.2 mm Hg, respectively. For AVA, the strongest determinants were valve sheath size, LVEF, and aortic annulus mean diameter with an average increase in MAE calculated to be 0.02, 0.01, and 0.01 cm^2, respectively. The MAE values computed for each learning algorithm are listed for both pressure gradient and AVA test set predictions in Table 2. Figure 4, *A* and *B* provide the learning curves generated for the ANN trained with the optimal hyperparameters for the pressure gradient and AVA datasets, respectively. In addition, the hyperparameters for the optimal estimator determined for each learning algorithm are provided in Table E2.

DISCUSSION

A summary of the main findings for this novel analysis is as follows: (1) an MAE value of 3.0 mm Hg was obtained for AV pressure gradient predictions; (2) an MAE value of 0.45 cm^2 was obtained for AVA predictions; and (3) the valve sheath size was found to be the strongest predictor of pressure gradient and AVA.

The application of ML and AI-based learning models have become more prevalent in predicting patient outcomes for various interventions. Within the context of TAVR, learning algorithms have been developed to aid clinicians in selecting the optimal procedural method. One study developed a GBM model that outperformed the standard statistics-based $TAVI_2$ score and CoreValve score models given that the area under the curve calculated from the

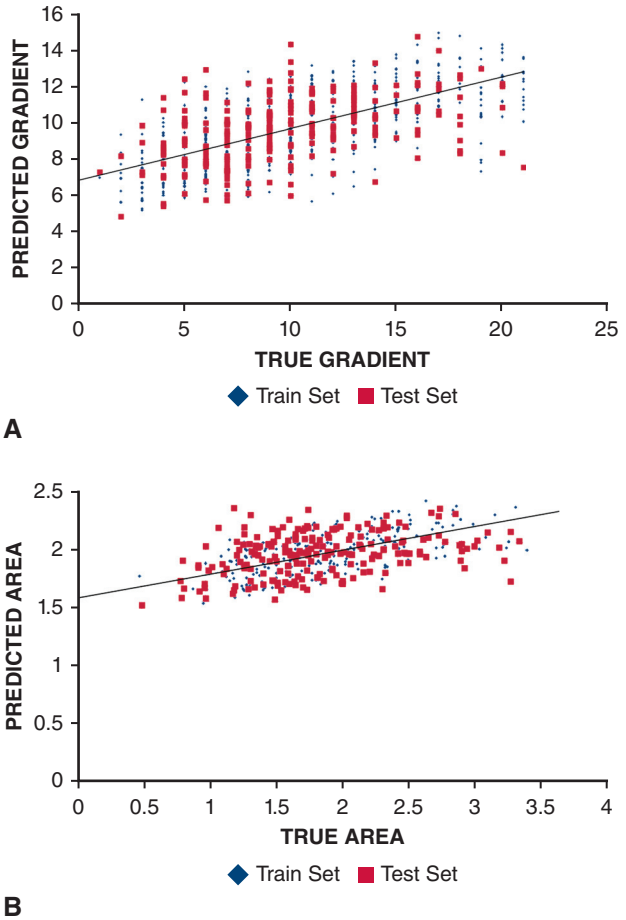

FIGURE 2. Predicted pressure gradient versus true pressure gradient (A) and predicted AVA versus AVA (B).

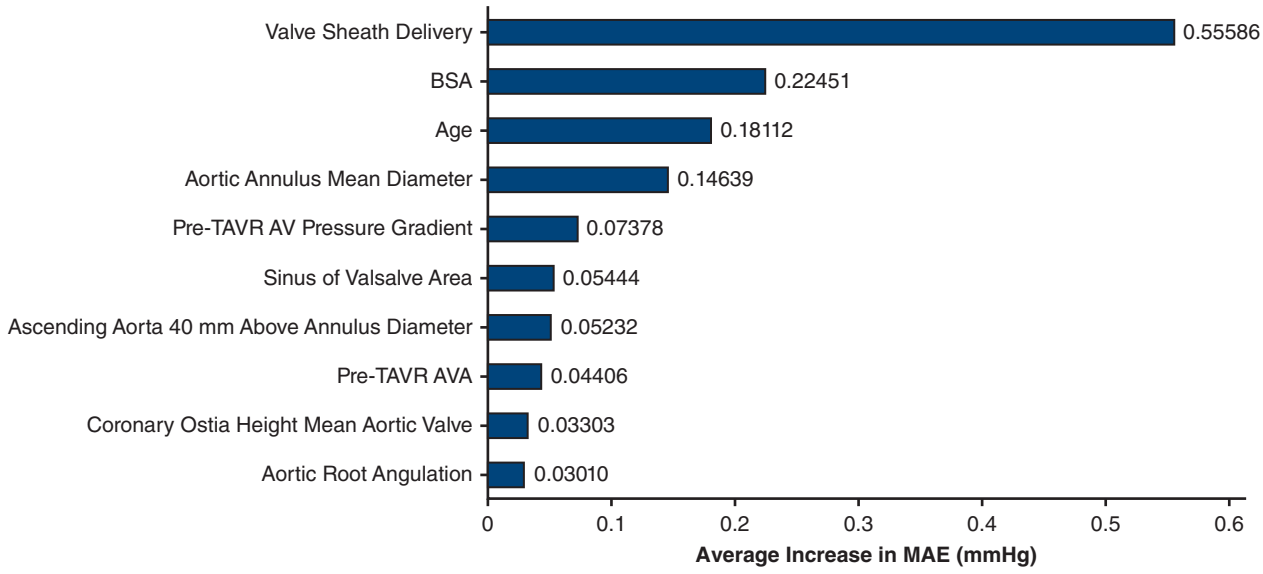

A

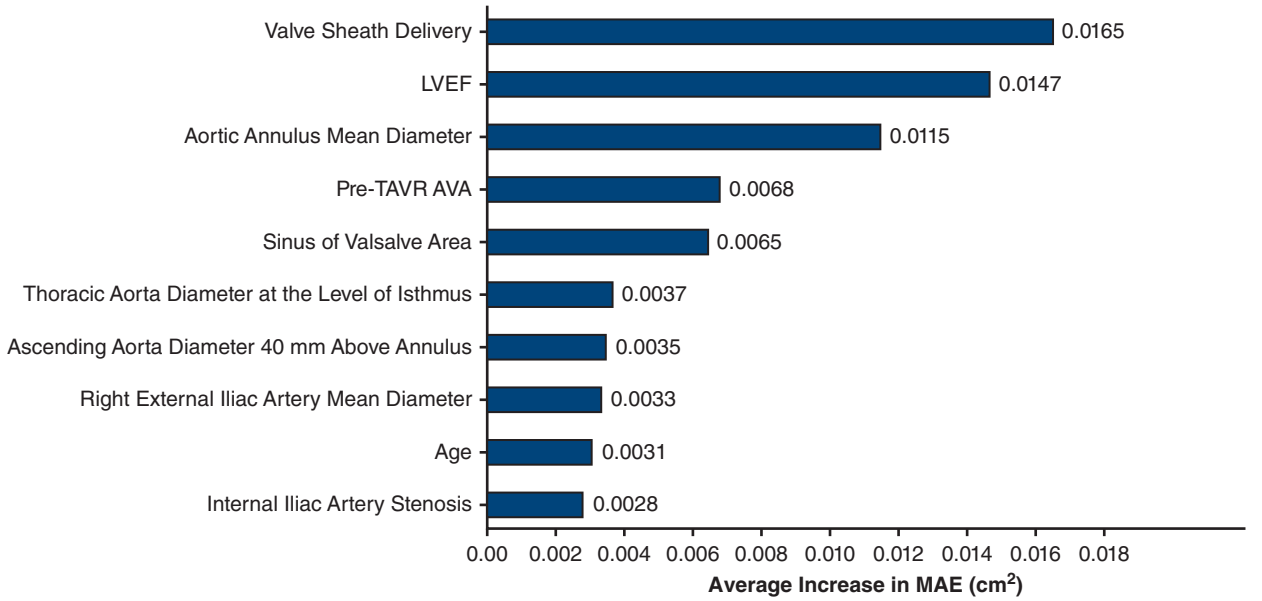

B

FIGURE 3. Top 10 input features with highest calculated feature importance for pressure gradient (A) and AVA (B) predictions. *BSA*, Body surface area; *TAVR*, transcatheter aortic valve replacement; *AV*, aortic valve; *AVA*, aortic valve area; *MAE*, mean absolute error; *LVEF*, left ventricular ejection fraction.

receiver operating characteristic curve was computed to be 0.72 for the GBM model versus 0.53 and 0.56 for the score models, respectively.[15] Interest has been shown in speculating the post-TAVR AV pressure gradient to aid preprocedural planning. Recently, a study applied a logistic regression model to predict the probability of developing a postoperative residual gradient greater than 20 mm Hg given a particular valve type subject to specified in vitro conditions.[20] The resulting area under the curve values for this study were reported to be 0.9465 and 0.9054 for Sapien 3 and Magna Ease valves, respectively.[20]

Although transvalvular pressure gradient and PPM have demonstrated unclear and complex relationships with post-TAVR outcomes, there is a consensus to minimize these effects. Specifically, a study investigating the impact of post-TAVR transvalvular pressure gradient on outcomes found higher mortality associated with lower postoperative echocardiographic gradients and higher invasive postoperative gradients.[11] Likewise, the nonlinearity of how PPM is related to clinical outcomes was analyzed in a 2021 study by Abbas and colleagues,[21] in which severe PPM was directly correlated with increased mortality in patients

TABLE 2. Calculated pressure gradient and aortic valve area mean absolute error for each learning algorithm

Variables	MAE pressure gradient	MAE AVA
SVR	Train: 2.9 mm Hg Test: 3.0 mm Hg	Train: 0.42 cm^2 Test: 0.45 cm^2
Elastic net regression	Train: 2.8 mm Hg Test: 3.0 mm Hg	Train: 0.40 cm^2 Test: 0.45 cm^2
MLP regression	Train: 2.7 mm Hg Test: 3.0 mm Hg	Train: 0.43 cm^2 Test: 0.45 cm^2
Random forest regression	Train: 2.7 mm Hg Test: 3.0 mm Hg	Train: 0.42 cm^2 Test: 0.45 cm^2
Gradient boosting regression	Train: 3.2 mm Hg Test: 3.2 mm Hg	Train: 0.41 cm^2 Test: 0.46 cm^2
Voting regression	Train: 2.7 mm Hg Test: 3.0 mm Hg	Train: 0.40 cm^2 Test: 0.45 cm^2

MAE, Mean absolute error; *AVA*, aortic valve area; *SVR*, support vector regression; *MLP*, multilayer perceptron.

with low flow post-TAVR and low ejection fraction post-SAVR. In this study, severe PPM in normal flow was not associated with poor clinical outcomes.[21] Although the post-TAVR pressure gradient may be insufficient to predict clinical outcomes, including PPM, decreasing the pressure gradient value remains an important objective because a higher gradient can result in increased stress on the prosthesis and heart failure.[22,23] Therefore, accurately predicting the postprocedural values for AV pressure gradient and AVA can potentially provide insight into how the selected TAVR approach can be further optimized during preprocedural planning. Considering the superior performance of learning models in cardiac interventions, we implemented AI-based learning algorithms to predict the mean AV pressure gradient and AVA from patient-derived CT data and postprocedure echocardiography.

Pressure Gradient and Aortic Valve Area Predictions

The calculated MAE values for the post-TAVR mean AV pressure gradient and AVA test predictions obtained from the final voting method were 3.0 mm Hg and 0.45 cm^2 (Table 2). All applied algorithms yielded consistent MAE values for the test set predictions, indicating the models' overall robustness and applicability to unseen datasets. In addition, the ANN learning curves generated for the training and validation sets (Figure 4, *A* and *B*) demonstrate good convergence as the training set size exceeds 500 patients and approaches 100% of its value, suggesting an optimized neural network structure. These observations further suggest that the final developed learning model does demonstrate potential in predicting these postoperative echocardiography measurements within a stable error range. A linear correlation between the predicted and true response variables is shown in Figure 2, *A* and *B*, where a

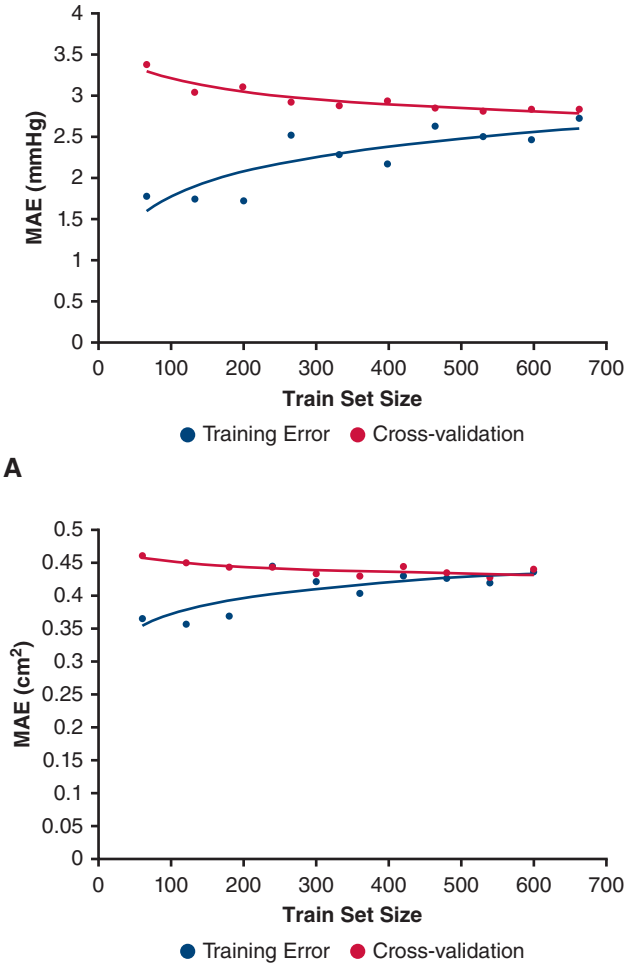

FIGURE 4. ANN learning curve generated for pressure gradient (A) and AVA (B) predictions. *MAE*, Mean absolute error.

constant distribution of predicted values can be seen across all true values.

On analysis of the permutation-based feature importance of each input variable, valve sheath size, BSA, and age were the strongest predictors of AV pressure gradient with an average increase in MAE computed to be 0.6, 0.2, and 0.2 mm Hg, respectively (Figure 3, *A*). For AVA predictions, the best determinants were identified to be the valve sheath size, LVEF, and mean aortic annulus diameter with an average increase in MAE calculated to be 0.02 cm^2 for the first feature and 0.01 cm^2 for the second and third variables (Figure 3, *B*). The fact that BSA and age were associated with pressure gradient is consistent with previous studies investigating predictors of postoperative pressure gradient.[24,25] Considering the major predictors identified from AVA predictions, the correlation between aortic annulus diameter and postprocedural AVA is expected because AVA and annulus measurements obtained from preprocedural CT are key variables used to assess the

severity of AS and anticipate TAVR outcomes.[26] Additionally, the association between LVEF and post-TAVR AVA may be due to an indirect correlation between LVEF and pre-TAVR AVA given how LVEF is often reduced in patients with severe AS.[27]

The main interesting result from analyzing feature importance was that the valve sheath size was identified as the strongest determinant for both postprocedural AV pressure gradient and AVA (Figure 3, *A* and *B*). Studies have shown that patients with femoral artery diameters less than the valve sheath size have a higher risk of vascular complications during transfemoral TAVR.[28,29] Reduced vessel diameters are usually due to heavy calcification of the vasculature, requiring increased minimal vessel diameters for valve sheath insertion.[30] From the correlation coefficients computed for all remaining input features after the preprocessing step for addressing multicollinearity, it was found that valve sheath size had the highest correlation with tortuosity ratings for the iliac and femoral arteries, which is consistent with the discussion provided in the review article. Specifically, these coefficients were 0.210 and 0.164 for external iliac artery tortuosity and common femoral artery tortuosity, respectively. Additionally, valve sheath size was found to have a comparable correlation with the sinus of Valsalva area (correlation coefficient = 0.147), which was identified to be one of the main predictors of postoperative AVA. The sinus of Valsalva area in turn had a moderate correlation with the annular area (correlation coefficient = 0.667). Therefore, our investigation points toward a tight indirect relationship between these features where the selection of smaller sheath sizes was correlated with smaller vasculature as well as annulus size, which is a risk factor for developing a higher postoperative pressure gradient and smaller EOA.[31] Although valve sheath delivery was found to be a dominant predictor of post-TAVR pressure gradient and AVA, this analysis also reveals the importance of considering all predictors (ie, STJ diameter or coronary ostia mean height) in constructing an overall accurate function that can predict the postoperative variables given the patient-specific cardiac input parameters.

Limitations

Factors that may have contributed to the final error values for pressure gradient and AVA predictions include the overall distribution of the dataset and the input features considered. In other words, the training set obtained after preprocessing for developing the learning models had a greater proportion of pressure gradient values near the average value (76%) compared with data points with pressure gradients less than 5 mm Hg or greater than 15 mm Hg (24%). Likewise, a smaller fraction of the training set for AVA predictions (33%) consisted of patients with post-TAVR AVA less than 1.50 cm^2 or greater than 0.75 cm^2, and the remaining data were between these 2 values (67%). Having a learning algorithm train on a dataset with an unequal distribution of output values may have resulted in a model more representative of data that dominates the training set. As a result, for both the pressure gradient and AVA predictions, there was strong agreement between the computed mean values for the true and predicted datasets, whereas the SDs differed significantly. For the pressure gradient predictions performed on the testing data, mean values were in close agreement (9.8 and 9.7 mm Hg for the true and predicted sets, respectively), whereas a large discrepancy between the SDs can be seen (4.2 and 1.9 mm Hg for the true and predicted sets). Likewise, the same distribution appears for AVA predictions where the mean values were computed to be 1.94 and 1.90 cm^2 for the true and predicted sets, and the resulting SD values were 0.59 and 0.14 cm^2, respectively. These results suggest that the model is limited to interpolating data within a narrow pressure gradient or AVA range, which would explain the high degree of scatter that can be noted in Figure 2, *A* and *B*.

In terms of how the input features may have contributed to the results, most of the variables investigated were preprocedural CT measurements of the patients' cardiac anatomy and vasculature or patient history (ie, pre-TAVR AVA, aortic root angulation, and aortic arch diameter) based on Table E1. Few features were related to the procedural method selected by the clinicians, such as valve sheath delivery, access site, and access method. Given the nature of these input features, it can be noted how this study has investigated predictors that indicate a potential predisposition toward presenting a higher residual pressure gradient or smaller AVA post-TAVR. Therefore, the scatter observed in Figure 2, *A* and *B*, demonstrate the correlation between the true and predicted response variable may have been due to a lack of intraprocedural variables from the dataset, such as valve type (Sapien vs Evolut) and valve size. Including procedural features, such as balloon- versus self-expandable and other valve properties, may aid in constructing a learning model that accounts for how the procedure itself contributed to the postoperative results. In addition, the input features lacked information regarding the invasive catheterization gradient during the time of TAVR, which can be a key intraprocedural variable to improve the model's predictive performance by revealing new insights into the discordance between invasive and echocardiographic-derived transvalvular pressure gradients.[32] Another major input feature lacking within the AI model is the granularity surrounding the patient-specific cardiac geometry, including left ventricular outflow tract morphology and calcium distribution. This can be a useful basis for future studies to improve the AI model by enabling image processing-based analysis of visualized patient-specific cardiac structures. Considering the limitations of

the overall study, although the AI model was internally validated, an external validation cohort was not included to assess the model's robustness or generalizability toward other patient populations. Therefore, future prospective studies must be performed to gauge the model's predictive performance on different datasets.

CONCLUSIONS

Our study found that applying AI learning models to predict post-TAVR pressure gradient and AVA using preprocedural CT measurements resulted in MAE values of 3.0 mm Hg and 0.45 cm^2, respectively. The consistency of these results across all learning models implemented demonstrates the robustness of the final constructed algorithm and overall predictive ability toward estimating postoperative transvalvular pressure gradient and AVA. Therefore, an implication of these findings is that these learning models can be used as an initial step toward optimizing preprocedural planning for TAVR given patient-specific cardiac anatomic features. Future studies can focus on building upon these AI models to account for the nonlinear and complex relationships among postoperative AV pressure gradient, AVA, and patient outcomes.

Conflict of Interest Statement

A.D. reports having patent applications filed on novel polymeric valves, vortex generators, superhydrophobic/omniphobic surfaces, and predicting leaflet thrombosis modeling. V.H.T. is a consultant for Abbott Vascular, Boston Scientific, Edwards Lifesciences, CryoLife, Shockwave, and JenaValve. A.D. and V.H.T. have filed a patent application on computational predictive modeling of thrombosis in heart valves. All other authors reported no conflicts of interest.

The *Journal* policy requires editors and reviewers to disclose conflicts of interest and to decline handling or reviewing manuscripts for which they may have a conflict of interest. The editors and reviewers of this article have no conflicts of interest.

References

1. Bleakley C, Monaghan MJ. The pivotal role of imaging in TAVR procedures. *Curr Cardiol Rep*. 2018;20:9.
2. Chamandi C, Puri R, Rodriguez-Gabella T, Rodés-Cabau J. Latest-generation transcatheter aortic valve replacement devices and procedures. *Can J Cardiol*. 2017;33:1082-90.
3. Joseph J, Naqvi SY, Giri J, Goldberg S. Aortic stenosis: pathophysiology, diagnosis, and therapy. *Am J Med*. 2017;130:253-63.
4. Gennari M, Rigoni M, Mastroiacovo G, Trabattoni P, Roberto M, Bartorelli AL, et al. Proper selection does make the difference: a propensity-matched analysis of percutaneous and surgical cut-down transfemoral TAVR. *J Clin Med*. 2021;10:909.
5. Otto CM, Kumbhani DJ, Alexander KP, Calhoon JH, Desai MY, Kaul S, et al. 2017 ACC expert consensus decision pathway for transcatheter aortic valve replacement in the management of adults with aortic stenosis: a report of the American College of Cardiology Task Force on clinical expert consensus documents. *J Am Coll Cardiol*. 2017;69:1313-46.
6. Sintek M, Zajarias A. Patient evaluation and selection for transcatheter aortic valve replacement: the heart team approach. *Prog Cardiovasc Dis*. 2014;56:572-82.
7. Mack MJ. Risk scores for predicting outcomes in valvular heart disease: how useful? *Curr Cardiol Rep*. 2011;13:107-12.
8. Généreux P, Piazza N, Alu MC, Nazif T, Hahn RT, Pibarot P, et al. Valve academic research consortium 3: updated endpoint definitions for aortic valve clinical research. *J Am Coll Cardiol*. 2021;77:2717-46.
9. Pibarot P, Dumesnil JG. Hemodynamic and clinical impact of prosthesis-patient mismatch in the aortic valve position and its prevention. *J Am Coll Cardiol*. 2000;36:1131-41.
10. Dayan V, Vignolo G, Soca G, Paganini JJ, Brusich D, Pibarot P. Predictors and outcomes of prosthesis-patient mismatch after aortic valve replacement. *JACC Cardiovasc Imaging*. 2016;9:924-33.
11. Khalili H, Pibarot P, Hahn RT, Elmariah S, Pilgrim T, Bavry AA, et al. Transvalvular pressure gradients and all-cause mortality following TAVR: a multicenter echocardiographic and invasive registry. *JACC Cardiovasc Interv*. 2022;15:1837-48.
12. Pibarot P, Salaun E, Dahou A, Avenatti E, Guzzetti E, Annabi MS, et al. Echocardiographic results of transcatheter versus surgical aortic valve replacement in low-risk patients: The PARTNER 3 Trial. *Circulation*. 2020;141:1527-37.
13. Bleiziffer S, Rudolph TK. Patient prosthesis mismatch after SAVR and TAVR. *Front Cardiovasc Med*. 2022;9:761917.
14. Pibarot P, Magne J, Leipsic J, Côté N, Blanke P, Thourani VH, et al. Imaging for predicting and assessing prosthesis-patient mismatch after aortic valve replacement. *JACC Cardiovasc Imaging*. 2019;12:149-62.
15. Agasthi P, Ashraf H, Pujari SH, Girardo ME, Tseng A, Mookadam F, et al. Artificial Intelligence Trumps TAVI(2)-SCORE and CoreValve Score in predicting 1-year mortality post-transcatheter aortic valve replacement. *Cardiovasc Revasc Med*. 2021;24:33-41.
16. Hernandez-Suarez DF, Kim Y, Villablanca P, Gupta T, Wiley J, Nieves-Rodriguez BG, et al. Machine learning prediction models for in-hospital mortality after transcatheter aortic valve replacement. *JACC Cardiovasc Interv*. 2019;12:1328-38.
17. Kilic A. Artificial intelligence and machine learning in cardiovascular health care. *Ann Thorac Surg*. 2020;109:1323-9.
18. Shouval R, Bondi O, Mishan H, Shimoni A, Unger R, Nagler A. Application of machine learning algorithms for clinical predictive modeling: a data-mining approach in SCT. *Bone Marrow Transplant*. 2014;49:332-7.
19. Altmann A, Toloşi L, Sander O, Lengauer T. Permutation importance: a corrected feature importance measure. *Bioinformatics*. 2010;26:1340-7.
20. Vogl BJ, Darestani YM, Crestanello JA, Lindman BR, Alkhouli MA, Hatoum H. A preliminary study on the usage of a data-driven probabilistic approach to predict valve performance under different physiological conditions. *Ann Biomed Eng*. 2022;50:941-50.
21. Abbas AE, Ternacle J, Pibarot P, Xu K, Alu M, Rogers E, et al. Impact of flow on prosthesis-patient mismatch following transcatheter and surgical aortic valve replacement. *Circ Cardiovasc Interv*. 2021;14:e012364.
22. Playford D, Stewart S, Celermajer D, Prior D, Scalia GM, Marwick T, et al. Poor survival with impaired valvular hemodynamics after aortic valve replacement: The National Echo Database Australia Study. *J Am Soc Echocardiogr*. 2020;33:1077-86.e1.
23. Søndergaard L, Ihlemann N, Capodanno D, Jørgensen TH, Nissen H, Kjeldsen BJ, et al. Durability of transcatheter and surgical bioprosthetic aortic valves in patients at lower surgical risk. *J Am Coll Cardiol*. 2019;73:546-53.
24. Algarni KD, Hassan E, Arafat AA, Shalaby MA, Elawad HH, Pragliola C, et al. Early hemodynamic profile after aortic valve replacement - a comparison between three mechanical valves. *Braz J Cardiovasc Surg*. 2021;36:10-7.
25. Bugani G, Pagnesi M, Tchetchè D, Kim WK, Khokhar A, Sinning JM, et al. Predictors of high residual gradient after transcatheter aortic valve replacement in bicuspid aortic valve stenosis. *Clin Res Cardiol*. 2021;110:667-75.
26. Ahn Y, Choi SJ, Lim S, Kim JB, Song JM, Kang DH, et al. Classification of severe aortic stenosis and outcomes after aortic valve replacement. *Sci Rep*. 2022;12:7506.
27. Ito S, Miranda WR, Nkomo VT, Connolly HM, Pislaru SV, Greason KL, et al. Reduced left ventricular ejection fraction in patients with aortic stenosis. *J Am Coll Cardiol*. 2018;71:1313-21.

28. Hayashida K, Lefèvre T, Chevalier B, Hovasse T, Romano M, Garot P, et al. Transfemoral aortic valve implantation new criteria to predict vascular complications. *JACC Cardiovasc Interv.* 2011;4:851-8.
29. Toggweiler S, Gurvitch R, Leipsic J, Wood DA, Willson AB, Binder RK, et al. Percutaneous aortic valve replacement: vascular outcomes with a fully percutaneous procedure. *J Am Coll Cardiol*. 2012;59:113-8.
30. Ramlawi B, Anaya-Ayala JE, Reardon MJ. Transcatheter aortic valve replacement (TAVR): access planning and strategies. *Methodist Debakey Cardiovasc J*. 2012;8:22-5.
31. Watanabe Y, Kozuma K. Transcatheter aortic valve implantation for patients with smaller anatomy. *Interv Cardiol*. 2015;10:155-7.
32. Barker M, Abbas AE, Webb JG, Pibarot P, Sathananthan J, Brunner N, et al. Standardized invasive hemodynamics for management of patients with elevated echocardiographic gradients post-transcatheter aortic valve replacement at midterm follow-up. *Circ Cardiovasc Interv.* 2022;15:e011243.

Key Words: AI, aortic stenosis, aortic valve, TAVR

APPENDIX E1. PREPROCESSING STEPS

Preprocessing Step 1: Removal of Specific Input Features

Some given features were filtered based on the percentage of missing data present as well as the relevance of predicting pressure gradient and AVA. Specifically, a feature was removed if more than 20% of the data were missing or involved unnecessary information, such as imaging protocol data (ie, scanner type, start/end phase, dose reduction algorithm), current medications, or billing information.

Preprocessing Step 2: Numerical Features

The resulting variables were then separated into numerical (ie, height and diameter values of anatomic features) and categorical (ie, calcium, stenosis, tortuosity, and dissection severity) types. For the numerical features, the average height and diameter were computed for the sinus of Valsalva, AV, and STJ. In other words, the sinus of Valsalva height measured at the right coronary cusp, left coronary cusp, and noncoronary cusp and sinus of Valsalva diameter measured at the right coronary cusp and left coronary cusp were averaged to obtain the mean sinus of Valsalva height and diameter, respectively. Likewise, the mean coronary ostia height and mean diameter were computed for the AV and STJ.

Preprocessing Step 2: Categorical Features

The data were first encoded by replacing "no" and "yes" or "unknown" with values of 0 or 1 for features, such as gender or relating to cardiac history and risk factors. Categories for race (White/Caucasian, Asian, Black/African American, Hawaii-Pacific, Multiracial, Other) were assigned values ranging from 0 to 6, respectively. The labels "tricuspid," "bicuspid," and "bioprosthetic" for indicating valve type were replaced with values 0, 1, and 2, respectively. One aspect to note about the risk factor input features is that the categories observed for history of smoking include "never," "former (>1 year)," and "current." These labels were encoded with values of 0, 1, and 2, respectively. Categorical variables for intraprocedural variables included access site and access method: access site options (femoral, transapical, subclavian, axillary, carotid, transcaval, and other) were imputed with values ranging from 0 to 6, and access method options (percutaneous, cutdown, minithoracotomy, and other) were given values spanning 0 to 3. The values "none," "mild," "moderate," "severe," and "occluded" for grading the severity of calcium, stenosis, tortuosity, and dissection for several access sites were assigned values of 0, 1, 2, 3, and 4, respectively. These access sites included the common iliac, external iliac, internal iliac, and common femoral arteries. For each access site, the severity values given for the calcium, stenosis, tortuosity, and dissection variables for the right and left components were summed, resulting in severity values ranging from 0 to 8 for stenosis and 0 to 6 for the remaining parameters.

Preprocessing Step 3: Training-Validation-Testing Split

The preprocedural and postprocedural data were then split into training, validation, and testing sets with a ratio of 3:1:1 to prevent data leakage that could occur during subsequent preprocessing steps.

Preprocessing Step 4: Addressing Outliers

After this data split step, outliers within each input numerical feature were eliminated by first computing the z-score values for the data provided for each variable and then removing any resulting values that lie outside 5 SDs from the mean. This step was performed twice for each data set to ensure the removal of all outlier CT measurement values. Outliers within the AVA and pressure gradient values for each dataset were removed by simply applying the interquartile range (IQR) method. The IQR method identifies data points as outliers if they fall within regions defined as $\leq$ (minimum value $-$ IQR) or $\geq$ (maximum value $+$ IQR). Applying this step resulted in the removal of patients with pressure gradients greater than 22 mm Hg and AVA values greater than 3.58 cm^2 or less than 0.30 cm^2.

Preprocessing Step 5: Addressing Missing Data

After eliminating outliers from the input and response variables for each dataset, any patients with no pressure gradient or AVA value recorded were removed, and any missing data for a given numerical input feature were imputed in a round-robin fashion using a Bayesian Ridge algorithm. This regression method develops a linear regression model by analyzing the probability distribution of the values for a specific feature as a function of the remaining input features. In addition, feature scaling was applied to all numerical features to ensure consistency in mean and SD values (mean $= 0$, SD $= 1$). On the other hand, missing values for each categorical variable were imputed with the most frequent values occurring for that feature.

Preprocessing Step 6: Eliminating Multicollinearity

The last preprocessing step applied to each dataset for the input features addressed the issue of multicollinearity where some input variables demonstrated high correlation. A Pearson correlation matrix was computed for the numeric variables, and variables corresponding to correlation values with magnitudes greater than or equal to 0.80 were removed. Likewise, a Kendall correlation matrix was used to remove highly correlated categorical variables. A Pearson correlation matrix was also calculated to quantify the correlation strength between the input features and the response variables. Any input features corresponding to correlation values with magnitudes less than or equal to 0.01

were eliminated because these values indicate very low correlation and therefore low predictive ability of the variables considered.

HYPERPARAMETER FINE-TUNING: REGRESSION

A detailed, technical description of how to implement each of the models listed below using Python can be found in the scikit-sklearn documentation.[E1]

Elastic Net Regression

The main model variables focused on included the regularization parameter "alpha" and the l1 ratio.[E2] The values of interest for the parameter alpha were defined to be 0.01, 0.05, 0.1, 0.5, and values ranging from 1 to 3. The l1 ratio variable was then assigned values ranging from 0.0 and 1.0.

Support Vector Regression

The hyperparameters that were varied for SVR[E3] included the kernel type, the regularization parameter "C," and the maximum acceptable error "epsilon." Linear, polynomial, radial basis function, and sigmoid kernels were tested. The parameter "C" was allowed to range from 0.1 to 5.0, and "epsilon" ranged from 0.01 to 6.0.

Random Forest Regression

The varied model hyperparameters included maximum depth for regulating the growth of the decision tree, minimum number of samples required to perform a split at each node, minimum number of samples remaining in each leaf node, and maximum number of features used to determine the best split.[E4] The values tested for the maximum depth were 2, 3, 5, 10, and 15, whereas values of 2, 10, 15, 20, 25, and 30 were for maximum samples per split. The values investigated for the minimum samples per leaf parameter included 1, 3, 5, 10, and 15. Different methods were then applied to calculate the maximum number of features. These methods included setting the hyperparameter to the total number of input features from the preprocedural dataset and computing the square root as well as the logarithm (base 2) of the number of input features. Because this method is an ensemble method, multiple estimators were built where individual predictions were averaged to form a final robust random forest regression model. The number of estimators was allowed to vary between 3 and 20 to ensure convergence of the training and validation results.

Gradient Boosting Regression

The gradient boosting method[E5,E6] involved the same hyperparameters as the random forest regressor because its function includes a decision tree, the same range of values was investigated for each hyperparameter. The number of estimators constructed with this ensemble method ranged from 3 to 20 to ensure agreement between the model's predictive performance for the training and validation sets. Additional features of this algorithm to note are the hyperparameter for specifying the loss function and the "alpha-quantile" value. During the training process, the loss function was set to "quantile," and estimators were built at "alpha-quantile" values of 0.05, 0.50, and 0.95. Implementing this step allowed for prediction intervals to be constructed since the 5th and 95th percentile predictions were outputted along with the actual predicted values at the 50th percentile.

Multilayer Perceptron Regression

For the ANN algorithm,[E7] the learning rate was first set to 0.001. The hyperparameters that were fine-tuned for the ANN algorithm include the number of neurons within the input layer ("hidden layer size") and the regularization term "alpha." For finding the optimal set of hyperparameters, the hidden layer size was defined as an array with sample values ranging from 300 to 500, and the array for "alpha" was set to values between 20 and 200. The combination of hidden layer size and "alpha" values that yielded the lowest MAE computed for the validation set was defined to be the optimal set of hyperparameters. After this fine-tuning process, the ANN for pressure gradient predictions was trained with a structure defined as an input layer with 49 neurons where each input neuron corresponds to an input feature, a single hidden layer with 425 neurons, and 1 output neuron for the pressure gradient estimation, yielding a total of 474. Likewise, for AVA predictions, the ANN structure was set as an input layer with 47 neurons, a single hidden layer with 375 neurons, and 1 output neuron for the predicted AVA, resulting in 423 neurons. The regularization hyperparameter "alpha" was set to a value of 50 and 20 for pressure gradient and AVA predictions, respectively, to prevent overfitting.

E-References

E1. Pedregosa F, Varoquaux G, Gramfort A, Michel V, Thirion B, Grisel O, et al. Scikit-learn: machine learning in Python. *J Mach Learn Res*. 2011;12:2825-30.

E2. Zou H, Hastie T. Regularization and variable selection via the Elastic Net. *J R Statist Soc B*. 2005;67:301-20.

E3. Smola AJ, Schölkopf B. A tutorial on support vector regression. *Stat Comput*. 2004;14:199-222.

E4. Svetnik V, Liaw A, Tong C, Culberson JC, Sheridan RP, Feuston BP. Random Forest: a classification and regression tool for compound classification and QSAR modeling. *J Chem Inf Comput Sci*. 2003;43:1947-58.

E5. Natekin A, Knoll A. Gradient boosting machines, a tutorial. *Front Neurorobot*. 2013;7:21.

E6. Friedman JH. Greedy function approximation: a gradient boosting machine. *Ann Stat*. 2001;29:1189-232.

E7. Rumelhart DE, Hinton GE, Williams RJ. Learning representations by back-propagating errors. *Nature*. 1986;323:533-6.

TABLE E1. Preprocedural, intraprocedural, and postprocedural variables extracted from dataset after preprocessing

Input variables (pressure gradient)	Input variables (AVA)	Output/response variables
Mean diameter aortic annulus	Mean diameter aortic annulus	AV pressure gradient
Ascending aorta diameter 40 mm above annulus	Ascending aorta diameter 40 mm above annulus	AVA
Aortic root angulation	Aortic root angulation	
Aortic arch diameter	Aortic arch diameter	
Mean diameter right common iliac artery	Thoracic aorta diameter at level of isthmus	
Mean diameter right common femoral artery	Thoracic aorta diameter at level of diaphragm	
Mean diameter right external iliac artery	Mean diameter right common iliac artery	
BSA	Mean diameter left common iliac artery	
Age	Mean diameter right common femoral artery	
Pre-TAVR AVA	Mean diameter right external iliac artery	
Pre-TAVR AV pressure gradient	LVEF	
LVEF	BSA	
Valve sheath delivery	Age	
Area sinus of Valsalva	Pre-TAVR AVA	
Sinus of Valsalva mean height	Valve sheath delivery	
Coronary ostia height mean AV	Sinus of Valsalva mean height	
STJ diameter mean thoracic aorta measurements	Area sinus of Valsalva	
Gender	Coronary ostia height mean AV	
Race	STJ diameter mean thoracic aorta measurements	
Commissural calcification	Gender	
Aortic annulus calcification	Race	
Aorto-mitral curtain calcification	Commissural calcification	
Aneurysm present in abdominal aorta	Aortic annulus calcification	
Dissection right common femoral artery	Aorto-mitral curtain calcification	
History of hypertension risk factors	Dissection right common femoral artery	
History of hyperlipidemia risk factors	History of Hypertension Risk Factors	
Family history of coronary artery disease risk factors	History of hyperlipidemia risk factors	
History of diabetes risk factors	Family history of coronary artery disease risk factors	
History of smoking risk factors	Menopause risk factors	
Family history of sudden cardiac death risk factors	History of diabetes risk factors	
Myocardial infarction cardiac history	History of smoking risk factors	
Moderate/severe valvular disease cardiac history	Family history of sudden cardiac death risk factors	
History of peripheral artery disease cardiac history	Myocardial infarction cardiac history	
Nonischemic cardiomyopathy cardiac history	History of peripheral artery disease cardiac history	
Chest pain symptoms	Congenital heart disease cardiac history	
Dyspnea symptoms	Nonischemic cardiomyopathy cardiac history	
Heart failure	Chest pain symptoms	
Transcatheter valve therapy access site	Transcatheter valve therapy access site	
Calcium common iliac artery	Stenosis common iliac artery	
Tortuosity common iliac artery	Calcium common iliac artery	
Dissection common iliac artery	Stenosis external iliac artery	
Stenosis external iliac artery	Calcium external iliac artery	
Calcium external iliac artery	Tortuosity external iliac artery	
Tortuosity external iliac artery	Dissection external iliac artery	

(Continued)

TABLE E1. Continued

Input variables (pressure gradient)	Input variables (AVA)	Output/response variables
Dissection external iliac artery	Stenosis common femoral artery	
Stenosis common femoral artery	Calcium common femoral artery	
Calcium common femoral artery	Stenosis internal iliac artery	
Tortuosity common femoral artery		
Stenosis internal iliac artery		

AVA, Aortic valve area; *AV*, aortic valve; *BSA*, body surface area; *TAVR*, transcatheter aortic valve replacement; *LVEF*, left ventricular ejection fraction; *STJ*, sinotubular junction.

TABLE E2. Best estimators identified for each learning algorithm applied for predicting pressure gradient and aortic valve area

	Best estimator – predicting pressure gradient	Best estimator – predicting AVA
SVR	C = 0.1, epsilon = 2.0, kernel = linear	C = 0.5, epsilon = 0.2
Elastic net regression	alpha = 0.1, l1 ratio = 0.2	alpha = 0.05, l1 ratio = 0.3
MLP regression	hidden layer size = 425, alpha = 50	hidden layer sizes = 375, alpha = 20
Random forest regression	max depth = 5, min samples split = 20, min samples leaf = 1, max features = auto	max depth = 2, min samples split = 2, min samples leaf = 1, max features = auto
Gradient boosting regression	alpha = 0.5, max depth = 15, min samples split = 30, min samples leaf = 1, max features = sqrt	alpha = 0.5, max depth = 10, min samples split = 20, min samples leaf = 1, max features = sqrt,

AVA, Aortic valve area; *SVR*, support vector regression; *MLP*, multilayer perceptron.